Proceedings of the Sixth International Conference on
Railway Technology: Research, Development and Maintenance
Edited by: J. Pombo
Civil-Comp Conferences, Volume 7, Paper 3.18
Civil-Comp Press, Edinburgh, United Kingdom, 2024
ISSN: 2753-3239, doi: 10.4203/ccc.7.3.18

Analysis of Aerodynamic Characteristics for High-Speed Maglev Train Operating Inside Tunnels at 600 km/h

S. Pan, L. Zhang, T. Lin, S. Xu and Y. Gao

School of Traffic & Transportation Engineering, Central South University, Changsha, China

Abstract

When the operating speed of the high-speed maglev train reaches 600 km/h, the aerodynamic drag and lift increase sharply, resulting in significant differences and larger variations in aerodynamic lift among the train cars. In scenarios such as entering and exiting tunnels or encountering other trains, the overturning moment, yaw moment, and pitch moment of the train significantly increase, sometimes even experiencing severe fluctuations. This not only seriously affects the stability of high-speed maglev train operation but also increases the difficulty of precise control of the suspension guidance system. In this study, based on the three-dimensional unsteady compressible Navier-Stokes equations and utilizing the k-epsilon turbulence model, we investigate the aerodynamic characteristics of Shanghai maglev trains with a 3-car formation operating at a speed of 600 km/h, both individually and during encounters while passing through tunnels. We analyze the peak and amplitude variations of aerodynamic drag, lift, and lateral forces for the entire train and different train formations, aiming to understand the aerodynamic behavior of high-speed maglev trains when operating inside tunnels. The research findings indicate that when two trains encounter each other compared to a single train passing through a tunnel, the maximum aerodynamic drag, lift, and lateral force of the entire train increase by 42.04%, 27.85%, and 625.45%, respectively. When a single train passes through, the aerodynamic drag, lift, and lateral force on the rear car are greater than those on the front car and greater than those on the middle car. When two trains encounter, the aerodynamic drag and lift on the rear car are greater than those on the front car and greater than those on the middle car, but the lateral force on the front car is greater

than that on the rear car and greater than that on the middle car. The research results can provide references for the development of high-speed maglev trains, the construction of maglev lines, and the control of train electromagnetic forces.

Keywords: high-speed maglev train, train/tunnel aerodynamics, tunnel aerodynamic effect, aerodynamic drag, entering and leaving tunnel, tunnel.

1 Introduction

Currently, breakthroughs have been made in maglev rail transit technologies both domestically and internationally, with multiple lines already in commercial operation. Maglev trains, along with high-speed EMU trains, have become advanced modes of transportation in modern rail transit. However, the continuous increase in the speed of maglev trains has also brought about numerous aerodynamic challenges, becoming a significant obstacle in the design and development of high-speed maglev trains.

When high-speed maglev trains operate at a speed of 600 km/h, they generate significant aerodynamic drag, lift, and lateral forces. Among these, aerodynamic drag accounts for over 90% of the total resistance, while aerodynamic lift can reach up to 40% of the train's weight, and aerodynamic lateral forces exceed 25% of the train's weight [1]. The aerodynamic forces distribution varies significantly among the different cars, resulting in considerable fluctuations in the train's roll, yaw, and pitch moments, leading to noticeable swaying of the carriages. This, in turn, reduces the stability of high-speed maglev train operations and increases the difficulty of adjusting the suspension guidance clearance. In extreme cases, it can lead to train-track collision accidents.

GAO et al. [2] conducted aerodynamic analysis on a 500 km/h maglev train during a straight-line encounter, revealing that the maximum pressure fluctuation occurs at the widest part of the train. HUANG et al. [3] studied the transient flow field generated when two maglev trains encounter each other at a speed of 430 km/h, analyzing the transient pressure changes on the train surface. MENG et al. [4] utilized overlapping grid technology to investigate the influence of streamline length on the aerodynamic characteristics of trains during straight-line encounters. They analyzed the flow patterns around the train body during encounters and the variation of train winds beside the track. Furthermore, the national standard 'Technical Standards for Maglev Railways (Trial)' [5] stipulates that the design of equipment and facilities inside tunnels should consider the effects of aerodynamic pressure but does not provide specific numerical values or further research. In conclusion, there is relatively limited research on the encounters of high-speed maglev trains at 600 km/h, with most focusing on the aerodynamic loads during straight-line segments, while studies on aerodynamic characteristics within tunnels are scarce.

Therefore, to improve the aerodynamic performance of high-speed maglev trains during tunnel operations and enhance the stability of train operations, this paper conducts detailed numerical simulations of the aerodynamic characteristics of single train and encounters passing through tunnels at a speed of 600 km/h on the Shanghai maglev train. This research aims to provide reference for the development of high-

speed maglev trains, the construction of maglev lines, and the control of train electromagnetic forces.

2 Methods

The computational model utilizes a 3-car formation of the Shanghai maglev train as shown in Figure 1(a), with the maglev train track model depicted in Figure 1(b). The calculation region for train passage through the tunnel is illustrated in Figure 2, aiming for a realistic simulation of the entire process. The initial calculation step is chosen at a distance of 50 meters from the entrance of the tunnel for the maglev train head.

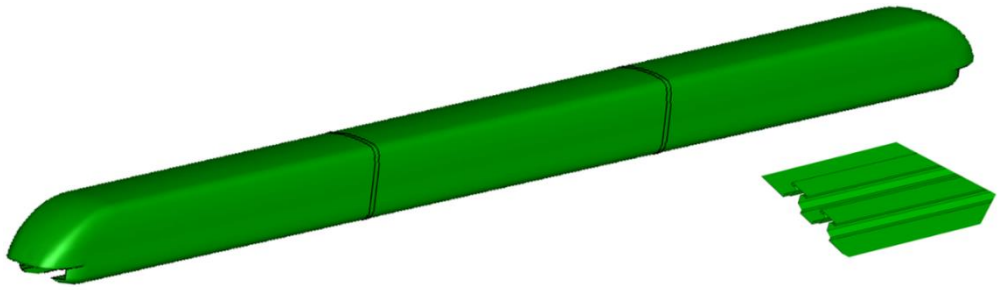

(a) The Shanghai Maglev Train Model (b) The Shanghai Maglev Track Model

Figure 1: Computational Model

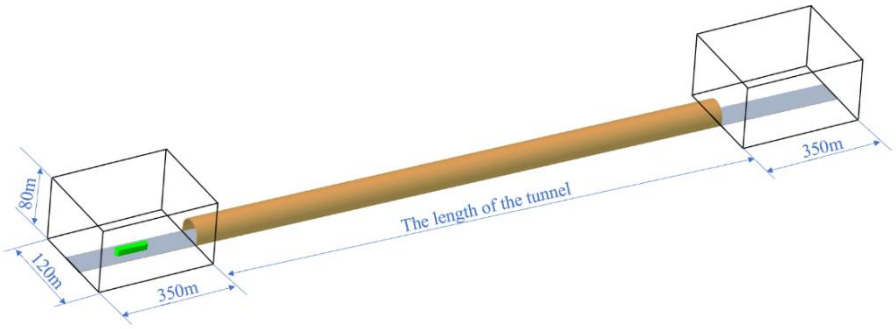

Figure 2: Computational Area for Maglev Train Passing through Tunnel

In this study, during the numerical calculations, the maglev train's speed is 600 km/h, resulting in a Mach number of 0.49. This necessitates considering the compressibility of the flow field. Additionally, as the train passes through the tunnel, the air within the tunnel undergoes rapid compression and expansion. Therefore, the calculations use a compressible ideal gas model, and the computational model employs the widely-used k-ε turbulence model.

When a train enters a tunnel at a certain speed, it causes compression waves and expansion waves to form inside the tunnel due to its compression of the air and the tunnel walls' restriction on the airflow. The propagation, reflection, and interference of these waves lead to significant unsteadiness in the air pressure inside the tunnel and the pressure on the train body over time. Simultaneously, the variation in air density resulting from the change in the flow field cannot be ignored. Therefore, during simulation calculations, the flow field should be partitioned into different zones. The calculation region for the train passing through the tunnel can be divided into six sub-

regions as shown in Figure 3. Region ① is the ground area, which typically requires simulating the boundary layer. Due to its elongated shape and very high aspect ratio, a structured mesh can be generated for this region. Region ② moves with the train and is closer to the train. The mesh can be slightly denser in areas closer to the train and relatively sparse in areas farther away from the train. Region ③ is a smaller area around the train, which moves with it. Because the train's shape is quite complex, this area generally uses unstructured mesh. Since the flow field near the train's surface is intricate, a very dense mesh is required in this area. To reduce mesh size, this region should not be too large. Regions ④ and ⑥ encompass most of the area outside the tunnel, including the far-field boundaries. Structured mesh can be used to divide this area. Region ⑤ is the area near the tunnel wall, which typically requires simulating the boundary layer. Due to its elongated shape and relatively large aspect ratio, a structured mesh can be generated for this region.

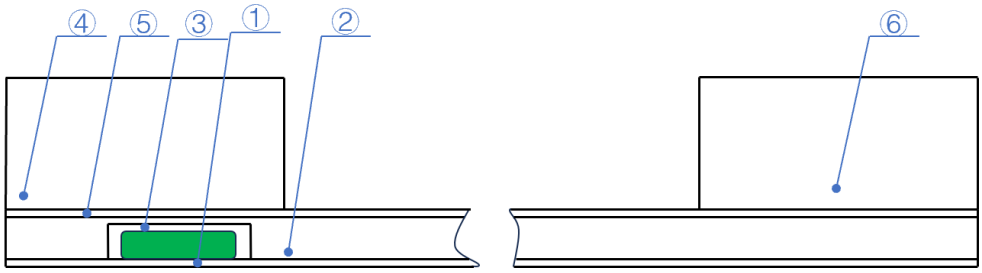

Figure 3: Schematic Diagram of Zoning for Train Passing through Tunnel Computational Domain

Next, to account for the relative motion between the train and the tunnel, when the train moves forward, regions ② and ③ move forward at the same speed as the train, while regions ①, ④, ⑤, and ⑥ remain stationary. The boundary between the stationary and moving regions is defined as the interface, and information exchange between stationary and moving regions is facilitated through this interface. The train passing through the tunnel involves information exchange between unstructured mesh regions, as well as between unstructured mesh regions and structured mesh regions. The information exchange between unstructured mesh regions and structured mesh regions is illustrated in Figure 4 below.

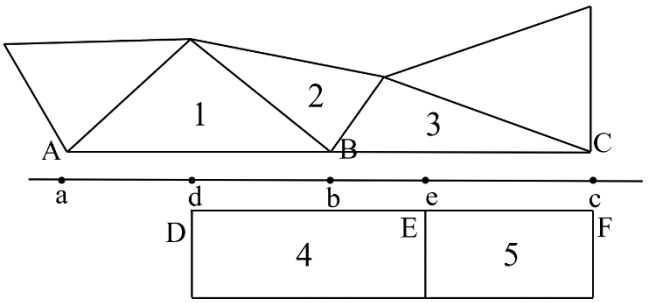

Figure 4: Schematic Diagram of Exchange Surface Information Exchange

The boundary interface of region ② is composed of ABC, while the boundary interface of region ⑤ is composed of DEF. During the calculation process, these two boundary interfaces slide relative to each other, forming the exchange surfaces: surfaces ABC and DEF, which intersect to create the common surface a-d-b-e-c; The boundary information of element 4 is provided through the surface d-b-e, interpolated from elements 1, 2, and 3. Simultaneously, the boundary information of elements 1, 2, and 3 is provided through the surface a-d-b-e-c, interpolated from element 4, element 5, and other boundary elements of region 5.

Finally, for the train surface, the following boundary conditions are specified: 1) The X-direction velocity component equals the given train velocity V, while the Y and Z-direction velocity components are set to 0; 2) No-slip boundary conditions are given for the lateral faces, top face, and bottom face of the domain; 3) Inlet boundary condition specifies a relative pressure of 0; 4) Outlet boundary condition specifies a relative pressure of 0; 5) Standard wall functions are used to simulate the tunnel wall surface. The numerical simulation conditions for the maglev train passing through the tunnel are presented in Table 1.

Table 1: Numerical Simulation Conditions for Aerodynamic Characteristics of Maglev Train Passing Through Tunnel

Vehicle Model	Formation	The area of the tunnel	Track gauge	The length of the tunnel	Vehicle speed
The Shanghai Maglev Train	3-car formation	140m^2	5.1m	Single car： 236m Double car： 161.16m	600km/h

3 Results

When the maglev train travels at a speed of 600 km/h through a double-track tunnel with an area of 140 m², the variations in aerodynamic drag, lift, and lateral force peaks and amplitudes are depicted in Figures 5, 6, and 7, respectively. Similarly, when the maglev train travels at 600 km/h and encounters another train at the midpoint of the double-track tunnel with an area of 140 m², the variations in aerodynamic drag, lift, and lateral force peaks and amplitudes are illustrated in Figures 5, 6, and 7, respectively.

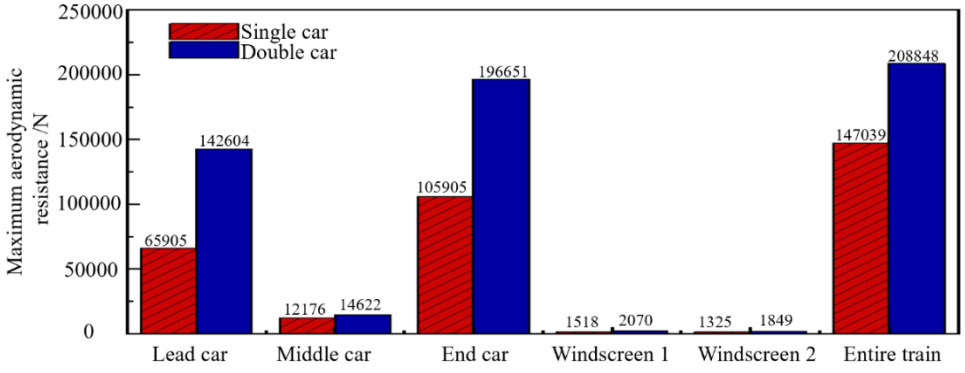

Figure 5: Aerodynamic resistance conditions in different parts of the train

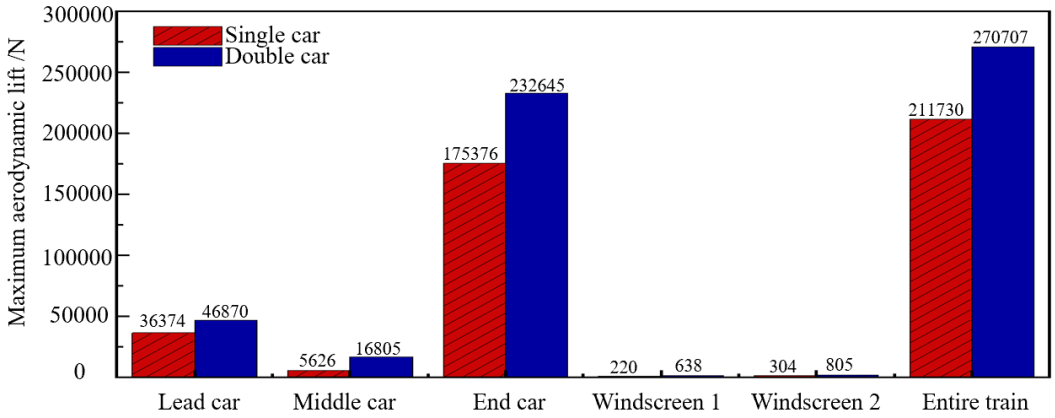

Figure 6: Aerodynamic lift conditions in different parts of the train

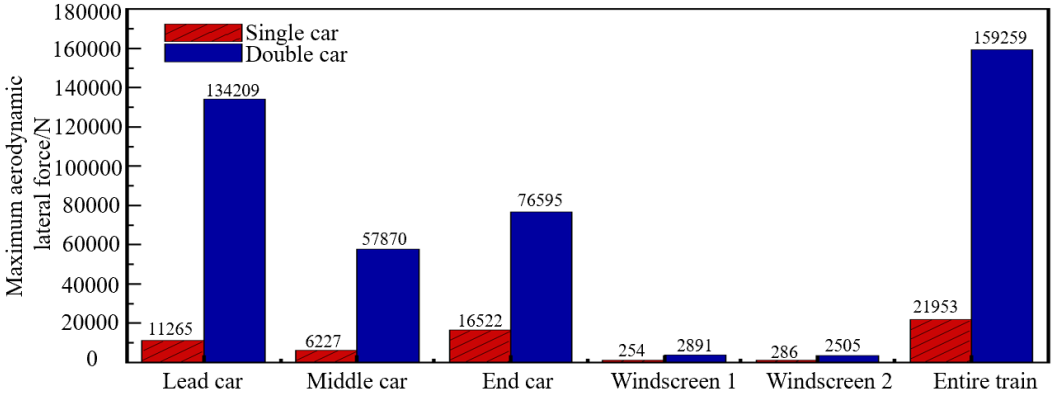

Figure 7: Aerodynamic lateral force conditions in different parts of the train

4 Conclusions and Contributions

Through computational analysis, the following conclusions are drawn: 1) During the train encounter process, the train is influenced by the leading train's headwind and wake, resulting in higher pressure and velocity in the surrounding flow field compared to a single train passing through. When a single train passes through, the maximum aerodynamic drag is 147,039 N, the maximum lift is 211,730 N, and the maximum lateral force is 21,953 N. During a double train encounter, the maximum aerodynamic drag is 208,848 N, the maximum lift is 270,707 N, and the maximum lateral force is 159,259 N. These values represent an increase of 42.04%, 27.85%, and 625.45%, respectively. 2) When a single train passes through, the rear car experiences higher aerodynamic drag, lift, and lateral force than the front car and the middle car. During a double train encounter, the rear car experiences higher aerodynamic drag and lift than the front car and the middle car, but the lateral force experienced by the front car is higher than that of the rear car and the middle car.

Acknowledgements

The authors acknowledge the computing resources provided by the High-speed Train

Research Center of Central South University, China. The research described in this paper was supported by the National Natural Science Foundation of China(52372369).

References

[1] S.-s DING, J.-l LIU, D.-w CHEN. Aerodynamic design of the 600 km/h high-speed maglev transportation system [J]. Experimental fluid mechanics, 2023, 37(1): 1-8.

[2] D.- g GAO, F NI, G.-b LIN. Aerodynamic Analysis of Pressure Wave of High-Speed Maglev Vehicle Crossing: Modeling and Calculation [J]. Energies, 2019, 12(19) : 1-18 .

[3] S HUANG, Z.-w LI, M.-z YANG. Aerodynamics of high-speed maglev trains passing each other in open air[J]. Journal of Wind Engineering and Industrial Aerodynamics, 2019, 188: 151−160.

[4] S MENG, S MENG, F WU, et al. Comparative analysis of the slipstream of different nose length-s on two trains passing each other[J]. Journal of Wind Engineering and Industrial Aerodynamics, 2021, 208: 104457.

[5] National Railway Administration. Maglev Railway Technical Standards (Trial) : TB 10630 − 2019 [S] . Beijing: China Railway Publishing House Co., Ltd., 2019.